ENHANCED QUANTUM EFFICIENCY OF PHOTO-INDUCED CARRIER GENERATION FOR PLASMA PCA BY EOT

Xiaolan LIU*[1], Yuan XU [2], Jingjing DU[3], Ruikai WANG[4]

The photoconductive antenna (PCA) is a kind of very typical THz sources at present. However, the poor radiation efficiency and power is the main drawback, limiting the further development and application of THz science and technology. THz waves generate anomalous transmission phenomena in porous planar structures with surface plasmonic polarization wave properties. The main factor that limits the quantum efficiency of photoconductive antennas at present is the limitation of the incident field strength. By exploiting the Extraordinary Optical Transmission (EOT), high field strengths can be generated at the photoconductive antenna electrodes, thus increasing the quantum efficiency of the photoelectric conversion and achieving the goal of improving the photoconductive antenna probe. In this study, in order to increase the photocurrent, a groove structure was used to enhance the local electric field of the grating electrode at the appropriate position of the grating. The effect of notch size, depth and location on transmittance was investigated, and the simulation results showed a clear enhancement effect of the local electric field, where the peak electric field reached 1.74×107 V/m. Being compared with the grating electrode with no grooves, the local electric field was increased by 4.07 times. By the constructed multi-physics model, the peak value of the improved PCA photocurrent is obtained to be 6.73 times higher than that of the conventional PCA. The simulation results show that quantum efficiency of Photo-Induced Carrier generation is improved by enhancing the local electric field on the semiconductor surface. By analyzing the influence of EOT of metal grating on the transmission field of THz PCA, a method to improve the radiation field of the PCA was given. This is significant in promoting the further application of THz.

Keywords: EOT; surface plasmon; semiconductor; multi-physics fields; quantum efficiency

1. Introduction

THz source is considered as a key part of THz science and technology. PCA has been one of the most widely used THz sources in recent years [1][2]. However, the further development and application of THz science and technology are limited

[1*]PhD, Dept. of Physics, Hengshui University, China, corresponding author, e-mail: liuxiaolan600465@163.com
[2] Lecturer, Dept. of Economics and Business administration, Hengshui University, China, e-mail: Greatlife123@163.com
[3] Lecturer, Dept. of Physics, Hengshui University, China, e-mail: jingjingguniang5@163.com
[4] Lecturer, Dept. of Physics, Hengshui University, China, e-mail: ruikaiw@163.com

by its low radiation efficiency and power [3][4]. Due to the low output power of THz radiation source, high background noise of thermal radiation in the frequency band range and severe attenuation of water vapor, the THz signal reflected back from the target is weak, which requires a THz detector with higher sensitivity and frequency resolution [5]. THz Time-Domain Spectroscopy (THz-TDS) is an important approach in THz detection technology [6]. The beam is split into two parts, one of which provides the phase delay through a translational segment. An optical pump pulse irradiates the emitter a THz pulse, which is focused on the detector after traveling a distance. The transients generated by THz induction can be detected from the probe pulse. The THz pulses are produced through the transient current of a PCA. In THz-TDS spectroscopy, the measurement of THz pulses is achieved by comparing the sampled results with the reference results [7].

The concept of PCA was first proposed by David Auston in 1984 [8]. He realized the generation of wide-band pulse THz wave based on an optically pumped PCA [9]. Since the distance between electrodes is small in the sub-wavelength metal structure PCA, the utilization of photogenerated carriers and the conversion quantum efficiency from an excited light to THz wave can be significantly improved. With the increasing progress of micro-nano processing technology and the continuous development of semiconductor materials, sub-wavelength metal structure terahertz PCA have gradually attracted more and more attention [10][11]. To avoid cancellation interference in the uncovered PCA, Awad et al. [12] proposed to etch the photoconductive material with every other gap based on the semiconductor processing process. Berry [13] confirmed that the transport path length of most photogenerated carriers could be shortened to the order of nanometer by using plasma contact electrodes similar to grating structures as illustrated in Fig. 1.

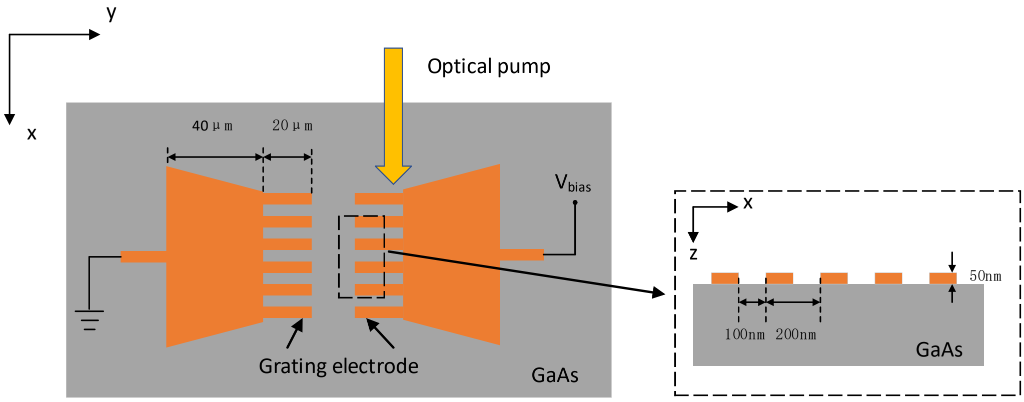

Fig. 1. Schematic diagram of metal grating electrode PCA

Additionally, it was claimed that the THz wave output power and the number of photogenerated carriers collected in sub-picosecond time can be increased, and the THz wave generation efficiency of PCA can be improved as well. One year later, Jooshesh [14] combined hexagonal metal nanostructure arrays with PCA. He intended to maximize the local current density and could increase THz waves intensity, generated by PCA, by more than 60%.

Since the THz-TDS determines THz radiation amplitude, the sampled dispersion can be obtained by the Fourier transform of the waveform [15]. The probe detection method based on the EOT of the PCA is able to break the diffraction limit. The increased sensitivity of the PCA requires an increase in the sensing current of the PCA. Great photoconductive current density requires ensuring stronger field strength so that the electro-optical conversion can obtain a large induced current. For THz band, EOT is usually produced due to SPP effect, and EOT increases the transmission field strength of semiconductor materials to obtain high sensitivity PCA probes. The research studies show that PCA technology based on surface plasma technology and nanotechnology is an efficient and economical way in THz generation and detection technology. In plasma PCA, the absorption of light quantum is improved by using semiconductors and the plasma irradiated by femtosecond laser pulses. The local electric field is enhanced, which can obviously enhance quantum efficiency of the THz emitter [16].

In this work, the influence of EOT on the transmission field of terahertz PCA was studied. Accordingly, a method to improve the radiation field of the PCA was given. The significance of this research is that it can be a guide for further improving the photoconductive current and the THz radiation ability of PCA. The main novelty and work of present study is as follows.

• Improve a method to the sensitivity of photoconductive antenna probe is proposed, which combines the EOT with the terahertz PCA technology.

• Calculate the dielectric properties of metals theoretically, through the Drude model. The dielectric properties of metallic silver are studied emphatically, and the dielectric constant formula of silver is simulated.

• Simulate the effect of notch size and specific location on the transmittance.

• Study the transmission field strength of PCA with modified subwavelength metal grating electrode structure in a semiconductor.

The remainder is organised as follows. Part 2 review and summarize related literature about photoconductive antennas and surface plasmon polaritons. Dielectric properties of metals and radiation characteristics of PCA are described Section 3. Simulations and numerical analysis of improved PCA are provided in Section 4. Section 5 compares and analyses the photogenerated current of several modified PCA. Part 6 summarized the paper.

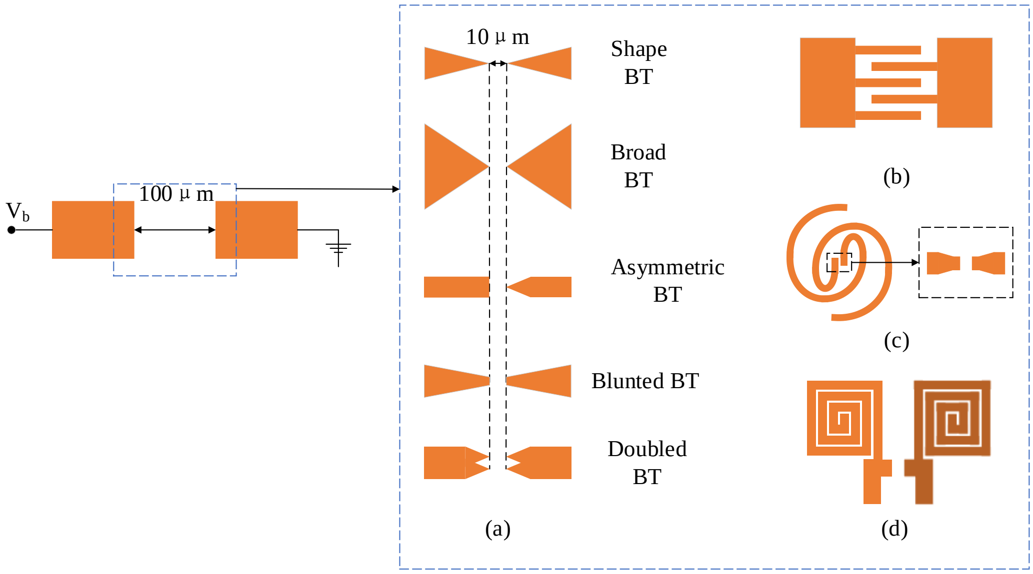

Fig. 2. Different electrode structures of PCA (a) different electrode structures of bow-tie antenna [18] (b) crossed-finger photoconductive antenna [19] (c) circular helical electrodes [20] (d) square helical electrode [21]

2. Related works

The electrode structure of the antenna in photo-conductive antennas is a key factor affecting the quantum efficiency of Photo-Induced Carrier generation. In recent years, scholars have studied and fabricated terahertz emitters with various electrode geometries, mainly deformations of dipole antennas, including rectangular, circular, and semicircular structures [17]. In addition to this, there are plasmonic nanostructures. It has been shown that a good shape of the electrode structure can greatly improve the performance of the antenna.

Alfihed et al. [18] investigated the radiation field amplitude and spectral bandwidth of Bow-Tie Antenna with different electrode structures, including a Sharp BT, a Broad BT, a Doubled BT in Fig. 2(a). For the Asymmetric BT structure, the normalized terahertz field amplitudes are 0.85, 0.89, and 1, while bandwidths are 3.7 THz, 3.5 THz,2.8 THz for Asymmetric BT, the Blunted BT structure, and the Broad BT structure, respectively. it is found that the Broad BT's amplitude and bandwidth are higher than Sharp BT. the Broad BT structure has a significant electric field singularity and the highest The Asymmetric BT structure has the widest bandwidth because of its lower capacitance.

The Fig. 2(b) indicates the crossed-fingered photoconductive antenna (IPCA) having a metallic nanostructure, as proposed by Boby et al. [19]. Including the output power of IPCA, an investigation of the size of the crossed-finger PCA and the impact of the input laser characteristics on the photocurrent, the quantum efficiency of light-to-terahertz conversion, and the bandwidth were conducted. Being the 44-element IPCA with a 20-nm finger width having the highest efficiency, the IPCA indicated an opt-THz conversion quantum efficiency of 0.1265%, a total current of 1.5404 A, and a conductance of 0.17155 V, as revealed by the results of simulation. With a higher electric field peak of 15.2 A/ps, the IPCA was shown to provide a larger bandwidth around 13.8 THz, as against that of the dipole PCA. The results being close to those of the dipole PCA, when the finger width was less than 20 nm, a decrease was observed in the effect of the IPCA.

When the orientation of the crystal of the GaAs substrates as Fig. 2(c) was changed, the parameters of the THz antennas could be substantially improved through the modification of the design of the planar circular helical electrodes, as demonstrated by Buryakov et al. [20]. Covering high and low frequencies of the emission spectrum, the terahertz radiated power output gets enhanced significantly by the combination of the logarithmic helical antenna, the plasmonic antenna, and the bow-tie antenna. That the frequency range and the output power of terahertz antenna are obviously impacted by the design of the electrode, was aptly demonstrated by Gholami et al. [21] through the simulation of a square helical electrode structure, as Fig. 2(d). Besides extending the frequency bandwidth of the terahertz radiation, its intensity is also increased by the use of multiple spirals in the electrode.

This paper proposes an improved metal grating electrode structure for PCA. Effectively adjust surface plasma waves using groove structures to achieve enhanced transmission field. In the grating electrode structure of a plasma PCA, a groove structure is taken at a suitable position to enhance the local electric field of the grating electrode. And using numerical simulation software to simulate the plasma PCA in multiple physical fields, it is concluded that the plasma PCA structure can enhance the transmission light intensity of semiconductor materials under diffraction limit conditions; It can significantly enhance the transmission field strength of semiconductor materials, thereby achieving greater photoconductive current and is expected to achieve strong terahertz radiation.

3. Methodology

3.1 Dielectric properties of metals

Most photoconductive antennas use semiconductor materials with short carrier lifetimes to suppress the additional DC component. However, high-density defects of the semiconductor materials can greatly affect the carrier mobility and quantum efficiency. Berry [22] proposed that the quantum efficiency can be greatly improved by using plasma photoconductive contact electrode technology. The plasma photoconductive contact electrode technique can, on the one hand, increase the transmission power of the laser, thus increasing the electric field energy for generating electron-hole pairs and increasing the carrier density. On the other hand, it can reduce the distance from the carriers to contact electrode, thus enhanced the radiation current of photoconductive antenna.

In the terahertz and optical bands, the properties of metallic materials can be described by the Drude model [23]. The German physicist Drude, to explain the transport performance of electrons, proposed a dispersion model, which approximates the electrons in metals as a gas, assuming that the metal consists of free moving electrons and fixed immobile ions, and that the free electrons are the carriers of electrical conductivity. When there is an external electromagnetic field, the electrons oscillate violently and lose energy due to mutual collisions, which are described by the collision angular frequency γ. where ω_p is the intrinsic metal parameter, representing the metal plasma frequency. The relative permittivity $\varepsilon(\omega)$ of metal is a complex number, where the real part $\varepsilon_r(\omega)$ and imaginary part $\varepsilon_i(\omega)$ are:

$$\varepsilon_r(\omega) = 1 - \frac{\omega_p^2}{\omega^2+\gamma^2} \quad (1)$$

From the Drude model, it can be concluded from Eq. (1) that the complex permittivity is associated with the collision angle frequency, the plasma frequency and the incident wave frequency. When $\omega \to \infty, \varepsilon_r(\omega) \to 1, \omega = \omega_p, \varepsilon_r(\omega) = 0; \omega < \omega_p, \varepsilon_r(\omega) < 0$， the relationship between real part of relative dielectric constant of metals ε'_{rc} and the frequency ω is shown in Fig. 3 below。When the electromagnetic wave frequency is obviously higher compared to metal plasma frequency, the complex dielectric constant of the metal tends to be close to 1. This effectively ignores the effect of interband leap of electrons on the dielectric constant. This effect is negligible when the optical frequency is relatively low, but for most noble metals, it starts to become apparent when the photon energy is greater than 1eV.

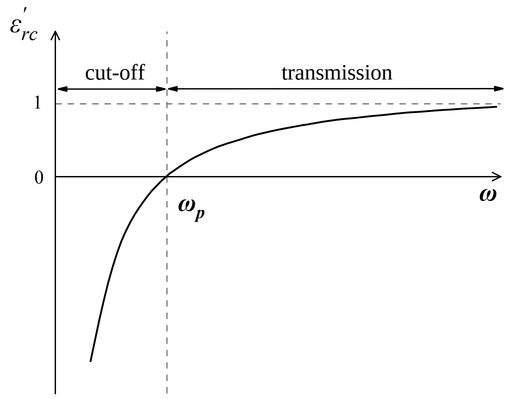

Fig. 3. Relation between real part and frequency of relative permittivity of metals

Silver (Ag) is one of the substances most used in surface plasma experiments, and its optical properties are crucial for theoretical predictions and experimental design. In plasmonic photoconductive antennas, the antennas are mostly made of silver (Ag). We take the experimental data from the literature [24-26], take their average values, and then fit the parameters of them to obtain:

$$\varepsilon(\omega) = \varepsilon_\infty \ \left(1 - \frac{\omega_p^2}{\omega^2 + i\omega\gamma}\right) \tag{2}$$

In Eq. (2), $\varepsilon_\infty = 4, \gamma_0 = 1.1088 \times 10^{14}$, $\omega_p = 6.6842 \times 10^{15} rad/s$. This data is used in the later analysis of metallic photoconductive antennas with metallic silver dielectric constants under laser irradiation.

3.2 Plasma electromagnetic mode on the surface of metal partition interface

Due to the special nature of the metal optical frequency dielectric constant, TM polarized light incident on the metal surface can excite surface plasmonic excitons when certain conditions are met. Generally, surface plasmon excitons are classified into two categories: Propagating Surface Plasmon Polaritons (PSPP) and Localized Surface Plasmon Polaritons (LSPP). The various types modes present at the metal/electrolyte interface. Propagating surface plasmonic excitons are conducted waves, which can be transmitted over a certain distance on a specially structured surface, while localized plasmonic excitons are non-conducting electromagnetic waves, which are bound around subwavelength dimensions and cannot propagate but can significantly enhance the local electric field, a property that is used in many fields such as surface-enhanced Raman scattering, spectral enhancement, and subwavelength imaging. As in Fig. 4, the electromagnetic field distribution of the transmitted wave in the metal can be described as follows, where the wave vectors in the medium and the metal are $k_1 = k_x \boldsymbol{e}_x + k_{1z}\boldsymbol{e}_z, k_2 = k_x \boldsymbol{e}_x + k_{2z}\boldsymbol{e}_z$。

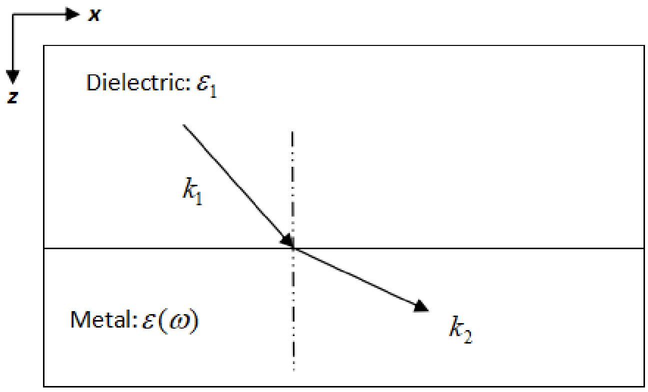

Fig. 4. Schematic diagram of the propagation between the metal and electrolyte partitions

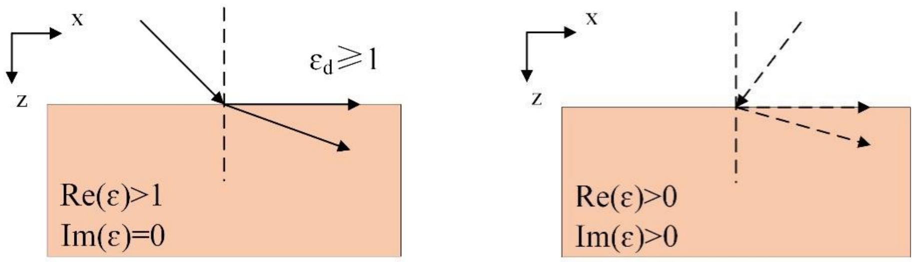

(a) (b)

Fig. 5. Brewster modes at the metal / electrolyte interface. (a) k_x is a real number; k_{1z}=+A$_1$, k_{2z}=+A$_2$; Re(k_{1z})>0, Im(k_{1z}) =0; Re(k_{2z})>0, Im(k_{2z}) =0. (b) k_x is a complex number; k_{1z}=+A$_1$, k_{2z}=+A$_2$; Re(k_{1z})>0, Im(k_{1z}) <0;.

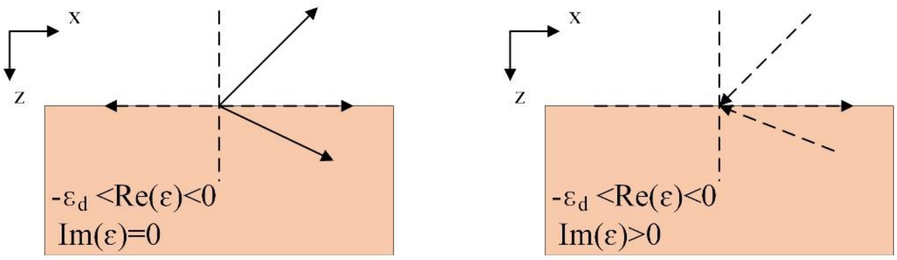

(a) (b)

Fig. 6. LSPP modes at the metal / electrolyte interface. (a) k_x is a pure imaginary number; k_{1z}=-A$_1$, k_{2z}=-A$_2$; Re(k_{1z})<0, Im(k_{1z}) =0; Re(k_{2z})>0, Im(k_{2z}) =0. (b) k_x is a complex number; k_{1z}=+A$_1$, k_{2z}=+A$_2$; Re(k_{1z})>0, Im(k_{1z}) <0; Re(k_{2z})>0 , Im(k_{2z}) <0.

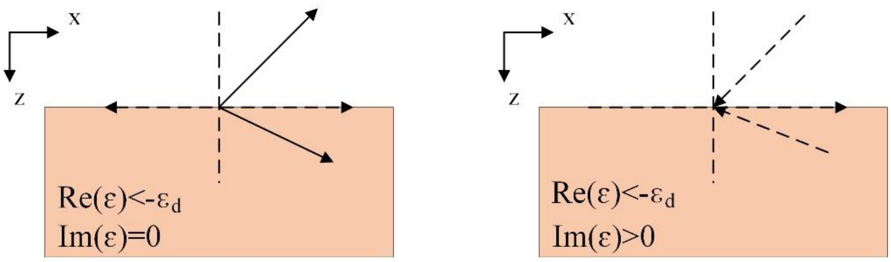

(a) (b)

Fig. 7. PSPP modes at the metal / electrolyte interface. (a) k_x is a pure imaginary number; k_{1z}=-A$_1$, k_{2z}=-A$_2$; Re(k_{1z}) =0, Im(k_{1z}) <0; Re(k_{2z}) =0, Im(k_{2z}) >0. (b) k_x is a complex number; k_{1z}=+A$_1$, k_{2z}=+A$_2$; Re(k_{1z})>0, Im(k_{1z}) <0.

$$\boldsymbol{H_2} = (H_y \boldsymbol{e}_y)\, exp(\, ik_x x + ik_{2z} z) \quad (3)$$

$$\boldsymbol{E_2} = \frac{H_y}{\omega \varepsilon_0 \varepsilon_2} (k_{2z}\boldsymbol{e}_x - k_x \boldsymbol{e}_z)\, exp(\, ik_x x + ik_{2z} z) \quad (4)$$

Fig.5-7 exhibit the nature of each mode is dependent on the nature of the wave vector components. If the wave vector along that direction is real, then it is a transmitted wave. On the contrary, if the wave vector is imaginary, it is a swift wave, which decays exponentially in the direction. If this attenuation is much larger than the wavelength, it can be named as pseudo-propagation wave. If k_{1z} is a real number, then there is a transmission nature of electromagnetic waves in the medium, on the contrary if k_{1z} is a pure imaginary number, then there is a swift wave in the **Z** direction, and with the exponential nature of decay, eventually gradually tends to zero.

Consider first the ideal condition where the metal is non-absorbing and can in principle support the transmission of electromagnetic waves over an infinite distance. In practice, this cannot happen, because real metals always exhibit small absorption and are therefore strictly asymptotic. However, for real metals $|Re(\varepsilon)| >> |Im(k_x)|$, the absolute value of real part is much larger compared to the imaginary part, then the wave is transmitted over a relatively long distance with respect to the wavelength, and the amplitude is not significantly attenuated is called a pseudo-propagating wave. Then the three cases can be identified as ideal non-absorbing metals and extend it to real metals.

3.3 Radiation characteristics of PCA

Compared to terahertz sources based on nonlinear optical effects, photoconductive terahertz sources have a very high quantum conversion efficiency from optical to terahertz frequencies. Each absorbed photon can produce a pair of electron-hole pairs, and multiple terahertz photons can be produced when the carriers reach the photoconductive antenna, and the power efficiency of the PCA can, in theory, exceed 100%. However, ordinary photoconductive antennas have a very low quantum efficiency and therefore can only achieve a very low power efficiency [27]. The common photoconductive antenna quantum efficiency is very low because it is limited by the electromagnetic wave diffraction limit. In order to have high transmitted optical power, the gap spacing between two metal electrodes needs to be a few microns in size. In general light-absorbing semiconductor materials, the carrier drift rate is generally at 10^7 cm/s, so in sub-picosecond time, only few carriers can reach the terahertz antenna to radiate terahertz waves, and most of the carriers become the DC current component, which reduces the electric field between the electrodes and further reduces the acceleration of the generated carrier flow to the metal electrodes.

For the radiation model analysis and field strength calculation of photoconductive antenna, the drift-diffusion model was used to first analyze the photoconductive dipole antenna. With the deepening of research, the radiation mechanism can be better explained by the current transient impulse model. The radiation power and the formulas of near field and far field obtained from the current transient impulse model are as follows:

$$\boldsymbol{E}_{r-near}(t) = -\frac{\eta_0\sigma(t)}{\eta_0\sigma(t)+(1+\sqrt{\varepsilon})}\boldsymbol{E}_b \propto \frac{I_0}{(K+I_0)^2}\boldsymbol{E}_b \quad (5)$$

$$\boldsymbol{E}_{r-far}(t) = -\frac{1}{4\pi\varepsilon_0 c^2}\frac{\boldsymbol{A}}{Z}\frac{d\sigma(t)}{1+\frac{\sigma(t)\eta_0}{1+\sqrt{\varepsilon}}} \propto \frac{I_0}{(1+KI_0)^2}\boldsymbol{E}_b \quad (6)$$

$$\boldsymbol{P} = \frac{3e^2 a_e^2}{2c^3}\gamma^4 \quad (7)$$

Where η_0 is wave impedance in the air, ε is a photoconductor relative dielectric constant, ε_0 is vacuum dielectric constant, conductivity of $\sigma(t)$ represents photoconductor, e refers to electronic charge, a_e expresses the surface electron acceleration of the light conductor, z is the measurement point distance, γ is carrier motion relative coefficient, A is the laser pulse irradiation area.

The magnitude of the photocurrent determines the strength of the terahertz radiation of PCA. According to the principle of photogenerated current generation, a femtosecond laser pulse is focused into the gap between the two electrodes of the photoconductive antenna, and when the laser pulse has a wavelength approximately equal to the semiconductor band gap, electrons from the semiconductor substrate jump from valence band to conduction band, and carried was generated. The charge makes accelerated motion in the bias electric field to form a transient photocurrent, which radiates terahertz waves. The factors that generally affect the transient photocurrent can be put roughly into three categories of laser-related parameters, including laser power, pulse width, etc., bias voltage and carrier lifetime, mobility. The photocurrent, impedance and phototransfer efficiency in the gap of a photoconductive antenna can be expressed as:

$$I = \frac{eV_b\mu_e\tau\eta_L P_L}{hf_L l^2} \quad (8)$$

$$R \approx \frac{hcf_R l^2}{\eta_L e\mu_e P_L\lambda_L} \quad (9)$$

$$\eta_{LE} = \frac{eV_b^2\mu_e\tau^2\eta_L f_R}{hf_L l^2} \quad (10)$$

where P_l is the incident laser power, l refers to gap length, V_b is the bias voltage, μ_e is the free carrier mobility, τ represent photocurrent decay time, η_L refer to laser illumination efficiency, c is light speed constant, λ_l is the laser wavelength, and f_R refer to laser repetition frequency.

4. Plasma PCA model base on EOT

4.1 Groove slit structure model

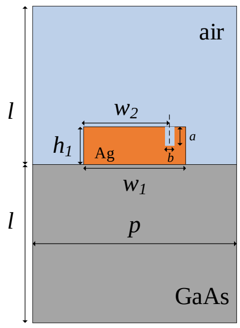

Fig. 8. Open-notched rectangular grating electrode model

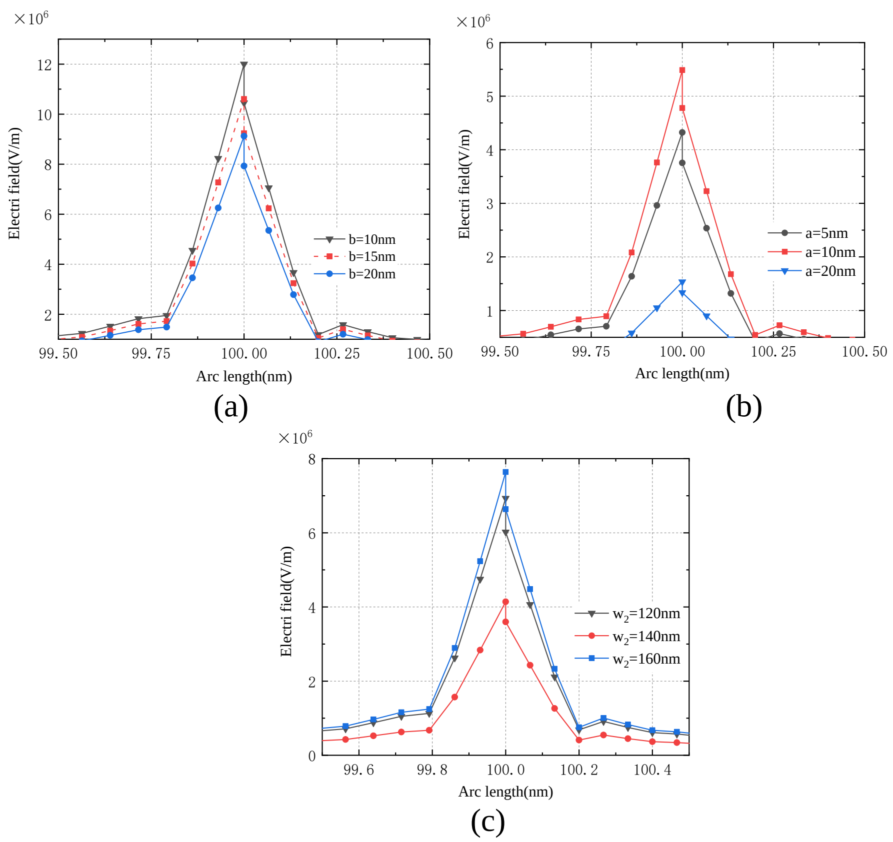

Fig. 9. Electric field distribution curves at metal and semiconductor interfaces.

In classical optics, the refraction, reflection and diffraction of light by a medium can be explained by the fluctuation of light, and the causes can all be attributed to the dielectric oscillator driven by external light waves and then radiating (scattering) light waves. The same generalized diffraction law can be extended to the role of the structural unit of a hypersurface in scattering external light waves. The realization of anomalous diffraction following the generalized diffraction law using a hypersurface can be applied to modulate the surface iso-excitations. The surface equiaxed excitations originate from the oscillation of conduction band electrons near the Fermi surface driven by the external electromagnetic field, and this collective oscillation behaviour can effectively transfer the electromagnetic field energy into the collective vibration energy of the electrons on the metal surface.

Leading to the phenomenon of an anomalous transmission and the enhancement of the interference between the incident waves in the slit and the surface plasma waves, the transmission of the surface plasma waves could be regulated by the hole and notch structure. Thus, the local electric field of grating electrode could be increased through the notch structure at proper location and the grating electrode structure of the plasmonic light-guided antenna. Considering 12.9 as the dielectric constant of GaAs and -32-i*0.7 as the dielectric constant of silver at 800 nm, Fig. 8 illustrates the silver with thickness 30nm, an 800 nm Gaussian beam being incident vertically to the grating electrode, and the model of the plasma PCA structure. The simulation provides the total field calculation while considering the duty cycle w_1/p as 0.5, the grating width w_1 as 200nm, and the grating period p being 400nm. With the two sides representing the conditions of the period boundary, the simulations provided the total field calculation.

To investigate the influence of notch on transmission, the effect of notch size and notch position on transmission is simulated and analyzed in this paper. In Fig.9, the notch structure at a suitable location can enhance the local electric field of the grating electrode in the structure of plasma light-guided antenna. The obtained peak electric field, as a known parameter, is input into the photoconductive multi-physics coupling solution model to obtain the photocurrent curve. The photoconductive current is used as the excitation current of the photoconductive antenna to study the sensitivity of the photoconductive antenna probe.

4.2 Improvement of sub-wavelength grating electrodes

PCA contains a fast activation switch embedded in the antenna structure. The PCA often exhibits as the form of metal electrodes on substrate. A femtosecond laser pulse is focused into the gap between two electrodes of the photoconductive antenna, and when the laser pulse has a wavelength approximately equal to the semiconductor band gap, electrons from the semiconductor substrate jump from the valence band to the conduction band, and electron-hole pairs are created. The charges are accelerated in a bias electric field to form transient photocurrents that radiate terahertz waves, which are generated by the voltage between the metal electrodes in the gap [28]. These accelerated charges are recaptured in the subsequent picosecond time frame into the semiconductor strip structure, the effect of the femtosecond laser pulse is to excite transient currents in the electrode slits.

In a PCA, the time for the carriers to move to the metal electrode is an important factor in the power efficiency. To achieve terahertz radiation, the time from the carrier to the metal electrode is required to be less than the period of the terahertz wave. In conventional terahertz photoconductive antennas, light-absorbing semiconductor materials with short lifetime are used to achieve ultrafast carrier travel time, while decreasing distance between metal electrodes can also reduce the carrier transmission time. However, that also reduces the absorption of irradiated optical power. Compared to terahertz sources based on nonlinear optical effects, photoconductive terahertz sources have very high conversion quantum efficiency from optical to terahertz frequencies. However, most of the short carrier lifetime semiconductor materials are grown under some special conditions, and during the semiconductor generation process, many defects are generated, and these high-density defects can greatly affect the carrier mobility and quantum efficiency. In order to overcome the problem of low quantum efficiency, plasmonic photoconductive contact electrode technology is proposed, and it is experimentally demonstrated that adding a subwavelength structured metal grating structure to the photoconductive antenna can greatly increase the photoconductive antenna power.

Besides the effect of metal thickness on the magnitude of the photocurrent generation, the grating structure, and on the metal dielectric properties, this study focuses on the influence of the grating metal electrode on radiation field of the plasma photoconductive antenna. Under the condition of an 800 nm Gaussian beam incident vertically on the grating electrode, the simulation model of the PCA structure is displayed in Fig. 10. Table 1 indicates relevant parameters. With the periodic boundary conditions prevailing on both the sides, the simulation adopts the total field calculation. The simulation optimization results are based on the parameters selected by the simulation results.

Table 1

Design parameters of Metal Grating Structure.

Parameters	Symbol	Value(nm)
air chamber height	l	800
metal thickness	h_1	30
grating period	p	200
metal width	w_1	100
groove position parameters	w_2	170
groove depth	a	15
groove width	b	5
groove spacing	d	25
800 nm silver dielectric constant	ε_1	-32-i*0.7
dielectric constant of GaAs	ε_2	12.9

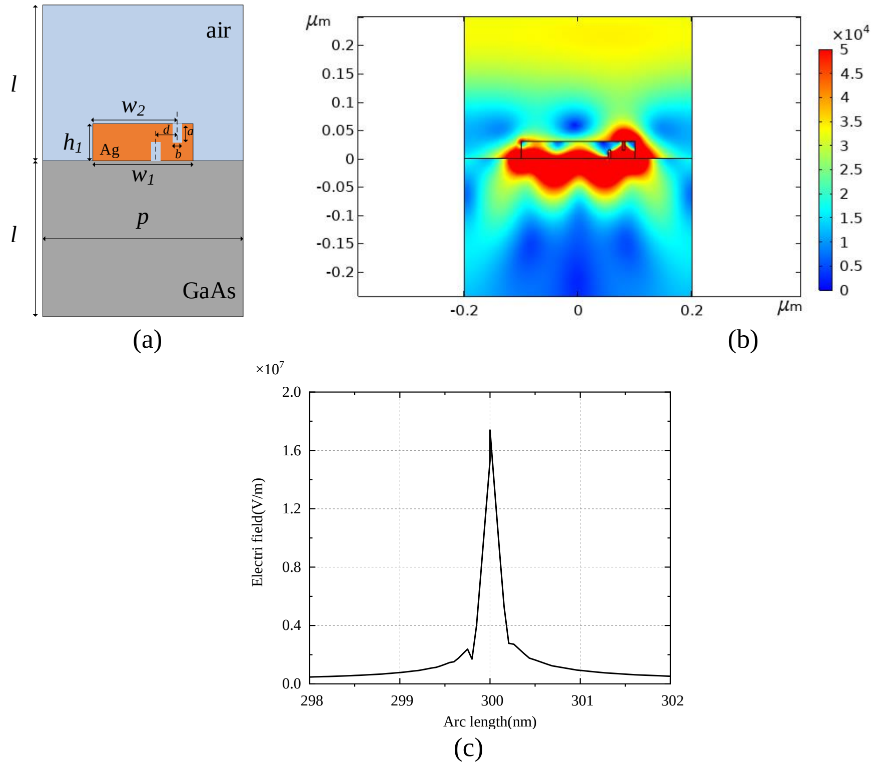

Fig. 10. Simulation results of grating electrode with open groove (a) grating electrode model with grooves on the upper and lower surfaces (b) surface magnetic field distribution result (c) Electric field distribution curves at metal and semiconductor interface

For the regulation of the transmitted waves, multiple positions are achieved through the creation of multiple grooves on the metal electrode. With 1.74×10^7V/m being the peak electric field value attained, the results of the simulation indicated that the effect of the local electric field enhancement was highly significant in case of the electrode structure with grooves on both the lower and upper surfaces. Whereas there was an increase by 4.07 times of the electric field of the grating electrode structure with grooves on both the lower and upper surfaces. There was an increase by a factor of 2.94 in the grooves on the upper surface, when compared with the grating electrode without grooves.

5. Multiphysics Simulation of Plasma PCA

The working mechanism of the photoconductive antenna is different from that of microwave antenna, involving multiple physical processes of photoelectric conversion, semiconductor diffusion, and electrostatic field distribution. The study uses multi-physics simulation techniques to investigate the mechanism of each physical field separately to achieve effective improvement of probe sensitivity.

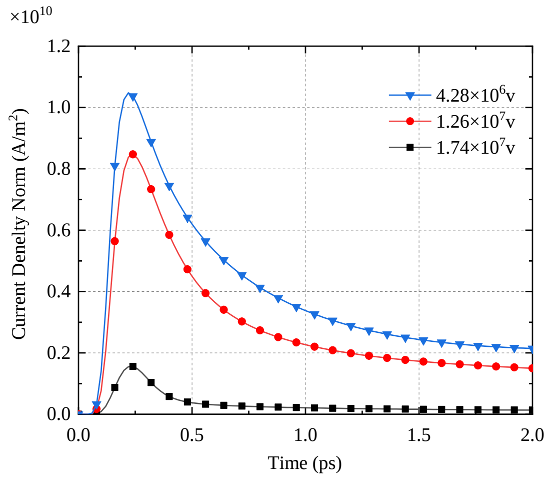

Fig. 11. Photocurrent contrast curve

Table 2

Simulation results of photoconductive antenna based on different metal electrode structures

Antenna	Peak electric field value	Current Density Norm(A/m^2)
Traditional Plasma PCA	4.28×10^6	1.56×10^9
Plasma PCA with grooves on the upper surface of the electrode	1.26×10^7	8.47×10^9
Plasma PCA with grooves on the top and bottom surfaces of the electrode	1.74×10^7	1.05×10^{10}

According to the above photoconductive antenna analysis, the RF and semiconductor modules in Multiphysics are used to construct a reasonable mathematical model, set the corresponding boundary and initial conditions, and use the solver to complete the numerical calculation of the conventional and plasma PCA. The peak electric field obtained in the previous section, as a known parameter, is input into a two-dimensional model for the coupled multi-physics field solution of the photoconductor to obtain the photocurrent curve, as in Fig.11.

Table 2 displays, through the grating structure, the plasma PCA structure can realize the enhancement of transmitted light intensity of semiconductor materials under the condition of less than diffraction limit, and the electric field enhancement effect is more significant by introducing the groove structure on grating electrode structure. The grating electrode structure with grooves on both upper and lower surfaces can increase the peak photocurrent by 6.73 times. The finite element method solver combines Maxwell equations, Poisson equations to simulate the process of terahertz radiation generation from PCA, which can be used to study and design more complex terahertz PCA compared with existing simulation methods.

6. Conclusions

The working mechanism of the photoconductive antenna is different from that of microwave antenna, involving multiple physical processes of photoelectric conversion, semiconductor diffusion, and electrostatic field distribution. The research uses multi-physics simulation techniques to study the mechanism of each physical field separately to achieve effective improvement of probe sensitivity. This paper mainly researched the anomalous transmission mechanism based on the notch structure and the design of a photoconductive antenna structure to enhance the transmitted light field. Based on the semiconductor diffusion equation, the generation of photoconductive currents in semiconductor structures is studied. The photoconductive current is used as the excitation current of the photoconductive antenna to study the sensitivity of the photoconductive antenna probe. In this work, high field strengths can be generated at the PCA electrodes base on EOT, thus improving the quantum efficiency of the photoelectric conversion for the purpose of enhancing the PCA probe. This work includes further reduction of the slit structure from microns to nanometer size and exploring the effect law of the interaction between multiple slit structures on the transmission field strength. The combination of EOT and PCA technology can break diffraction limit and achieve subwavelength spatial resolution, which has important function in target imaging, security detection, biological detection, and medical diagnosis.

Acknowledgments

This study has obtained the support of Hebei Natural Science Foundation (F2021111001) and Science and Technology Project of Hebei Education Department (BJ2020206).

REFERENCES

[1]. *G. Slekas, Z. Kancleris, A. Urbanowicz, and R. Ciegis,* "Comparison of full-wave models of terahertz photoconductive antenna based on ordinary differential equation and monte carlo method", European Physical Journal Plus, vol.135, no.1, 2020, pp.1-16.

[2]. *A. Saeed, O. Gurbuz and M. A. Akkas,* "Terahertz communications at various atmospheric altitudes", Physical Communication, vol.41, no.4, 2020, pp.101113.

[3]. *N. Arora, S. H. Gupta, and B. Kumar,* "Performance analysis of Terahertz communication link for cooperative Wireless Body Area Network", Optik International Journal for Light and Electron Optics, vol.3, no.1, 2021, pp.167376.

[4]. *H. Zhang, L. Shi and M. He,* "Extension of terahertz time-domain spectroscopy: a micron-level thickness gauging technology", Optics Communications, vol. 506, 2022, pp.127597.

[5]. *I.V. Minin, O. V. Minin, J. Salvador-Sanchez, J. D. Notario and Y. M. Meziani,* "Responsivity enhancement of a strained silicon field effect transistor detector at 03 thz using the terajet effect", Optics Letters, vol. 46, no.13, 2021, pp. 3061-3064.

[6]. *L. Hale, C. Harris, T. S. Luk, Addamane, J. Reno and I. Brener,* "Highly efficient terahertz photoconductive metasurface detectors operating at microwatt-level gate powers", Optics letters, vol. 46, no.13, 2021, pp. 3159-3162.

[7]. *H. Y. Mei, W. Xu, C. Wang, R. X. Yao and F. Liu,* "Magneto-optical properties of tri-layer graphene measured via terahertz time domain spectroscopy", Integrated Ferroelectrics, vol. 213, no. 1, 2021, pp.35-40.
[8]. *P. H. Siegel,* "Terahertz pioneer: david h. auston", Terahertz Science and Technology, IEEE Transactions on, vol.1, no.1, 2011, pp.6-8.
[9]. *B. Gowland,* "Review: moving against the system: the 1968 congress of black writers and the making of global consciousness by david austin", Race & Class, vol.61, no. 4, 2022, pp.105-107.
[10]. *T. M. Blessan, C. Venkateswaran and N. Yogesh,* "All-optical terahertz logic gates based on coupled surface plasmon polariton sub-wavelength waveguiding in bulk dirac semimetal", Optik, vol.257, 2022, pp.168795.
[11]. *S. T. Xu, F. Fan, H. Cao, Y. Wang and S. Chang,* "Liquid crystal integrated metamaterial for multi-band terahertz linear polarization conversion", Chinese Optics Letters, vol.19, 2021, pp.093701.
[12]. *M. Awad, M. Nagel and H. Kurz,* "LT-GaAs Based Photoconductive Antenna Arrays for Pulsed and CW Operation", Joint International Conference on Infrared Millimeter Waves & International Conference on Teraherz Electronics. IEEE, Shanghai, China, 2006, pp.49.
[13]. *C. W. Berry, M. Jarrahi,* "Terahertz generation using plasmonic photoconductive gratings", New Journal of Physics, vol. 14, no.10, 2012, pp. 105029.
[14]. *A. Jooshesh, L. Smith and M. Masnadi-Shirazi,* "Nanoplasmonics enhanced terahertz sources", Optics Express, vol.22, no.23, 2014, pp. 27992-28001.
[15]. *N. P. Brown, M. M. Eladl, A. M. Steinberg, J. A. Deibel and M. L. R. Walker,* "noninvasive thz-tds measurements of plasma bounded and optically shielded by hall thruster wall material", Plasma Sources Science and Technology, vol.30, no.7, 2021, pp.075027.
[16]. *A.I. Panas, S.G. Chigarev, E.A. Vilkov, O.A. Byshevski-Konopko, D.L. Zagorskiy, I.M. Doludenko,* "Relationship between Thermal and Dynamic Radiation in a Spin-Injection THz Emitter", Bulletin of the Russian Academy of Sciences: Physics, vol.86, no.7, 2022, pp. 841-845.
[17]. *Y. He, Y. Chen, L. Zhang, S. W. Wong and Z. N. Chen,* "An overview of terahertz antennas", China Communications, vol.17, no.7, 2020, pp.124-165.
[18]. *S. Alfihed, I. G. Foulds and J. F. Holzman,* "Characteristics of bow-tie antenna structures for semi-insulating gaas and inp photoconductive terahertz emitters", *Sensors,* vol.21, no.9, 2021, pp. 3131.
[19]. *E. N. F. Boby, P J. Rajapati, V. Rathinasamy, S. Mukherjee and S. Mondal,* "Parametric Investigation of Interdigitated Photoconductive Antenna for Efficient Terahertz Applications", ARABIAN JOURNAL FOR SCIENCE AND ENGINEERING, vol.47, 2022, pp.3597-3609.
[20]. *A. M. Buryakov, M. S. Ivanov, D. I. Khusyainov, A. V. Gorbatova and E. D. Mishina,* "Effects of crystallographic orientation of gaas substrate and the period of plasmon grid on thz antenna performance", Annalen der Physik, vol.533, no. 8, 2021, Article ID: 2100041 (7 pages).
[21]. *S. Gholami and A. Bahari,* "Enhancement of the intensity and bandwidth of terahertz radiation in photoconductive dipole antennas", Optical and Quantum Electronics, vol.53, no.4, 2021, pp.169.
[22]. *Berry, W. Chirstopher, Hashemi, R. Mohammad, M. Unlu, M. Jarrahi,* "Nanoscale contact electrodes for significant radiation power enhancement in photoconductive terahertz emitters", IEEE MTT-S International Microwave Symposium Digest, Seattle, WA, United states, 2013.
[23]. *P. F. Yang, J. Q. Yao and X. Wei,* "THz modulator based on the drude model", Optoelectronics Letters, vol.7, no.1, 2011, pp.19-21.
[24]. *P. B. Johnson and R. W. Christy,* "Optical constants of noble metals", Physical ReviewB, vol.6, no.12, 1972, pp.4370-4379.
[25]. *S. Babar and J. H. Weaver,* "Optical constants of Cu, Ag, and Au revisited", APPLIED OPTICS, vol.54, no.3, 2015, pp. 477-481.
[26]. *K. M. McPeak, S. V. Jayanti, S. J. P. Kress, S. Meyer, S. Iotti, A. Rossinelli and D. J. norris,* "Plasmonic films can easily be better: Rules and recipes", ACS Photonics, vol.2, no.3, 2015, pp.326-333.

[27]. *J. Sun, H. Cai, M. Li, Y. Xu, and Y. Liu,* "Enhancement effect on photoelectric conversion efficiency of plasmon-induced terahertz photoconductive antenna", Optik-International Journal for Light and Electron Optics, vol.227, no.10, 2021, pp.166021.
[28]. *L. Zhu, Y. Huang, C. He, Y. Wu, Y. Zhou, Z. Fan, J. Dong, K. Zhang and X. Xu,* "Transient anisotropic photocurrent induced terahertz emission from the surface of black phosphorus", physica status solidi (RRL): rapid research letterse, vol.11, 2021, pp.15.